Simultaneously increased strength and ductility via the hierarchically heterogeneous structure of Al-Mg-Si alloys/nanocomposite

Article *in* Materials Research Letters · April 2020

DOI: 10.1080/21663831.2020.1744759

Run Geng
Jilin University

Qinglong Zhao
Jilin University

Feng Qiu
Jilin University

Qi-Chuan Jiang
Jilin University

Taylor & Francis
Taylor & Francis Group

Materials Research Letters

ISSN: (Print) 2166-3831 (Online) Journal homepage: https://www.tandfonline.com/loi/tmrl20

Simultaneously increased strength and ductility via the hierarchically heterogeneous structure of Al-Mg-Si alloys/nanocomposite

Run Geng, Qinglong Zhao, Feng Qiu & Qichuan Jiang

To cite this article: Run Geng, Qinglong Zhao, Feng Qiu & Qichuan Jiang (2020) Simultaneously increased strength and ductility via the hierarchically heterogeneous structure of Al-Mg-Si alloys/nanocomposite, Materials Research Letters, 8:6, 225-231, DOI: 10.1080/21663831.2020.1744759

To link to this article: https://doi.org/10.1080/21663831.2020.1744759

MATER. RES. LETT.
2020, VOL. 8, NO. 6, 225–231
https://doi.org/10.1080/21663831.2020.1744759

MATERIALS RESEARCH LETTERS
Taylor & Francis
Taylor & Francis Group

ORIGINAL REPORTS

OPEN ACCESS Check for updates

Simultaneously increased strength and ductility via the hierarchically heterogeneous structure of Al-Mg-Si alloys/nanocomposite

Run Geng[a,b], Qinglong Zhao [a,b], Feng Qiu[a,b] and Qichuan Jiang[a,b]

[a]State Key Laboratory of Automotive Simulation and Control, Jilin University, Changchun, People's Republic of China; [b]Key Laboratory of Automobile Materials, Ministry of Education and School of Materials Science and Engineering, Jilin University, Changchun, People's Republic of China

ABSTRACT
The increase in strength usually accompanies with ductility loss in structural materials. We proposed a novel approach to the design and fabrication of hierarchically structured Al-Mg-Si alloys/nanocomposites with improved strength and ductility. The layered distribution of TiC nanoparticles (TiC_p), bimodal-sized grains and precipitates were produced in a laminated composite composed of Al-Mg-Si matrix alloy and TiC_p/Al-Mg-Si composite by accumulative roll bonding (ARB), increasing yield strength from 380 MPa to 443 MPa with a uniform elongation from 5.0% to 6.4%, compared to the ARB TiC_p/Al-Mg-Si composite. This work provides a new strategy for producing high strength composite sheets for industrial applications.

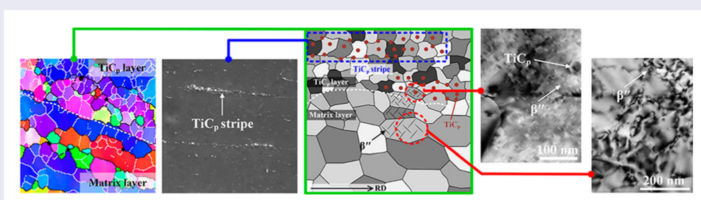

IMPACT STATEMENT
A hierarchical structure with the layered distribution of nanosized TiC particles (TiC_p) was obtained through the master alloy-casting process and accumulative roll bonding process. Significant improvement in strength was obtained with no loss in ductility.

ARTICLE HISTORY
Received 13 February 2020

KEYWORDS
Metal-matrix composites; nanocomposite; accumulative roll bonding; strength; ductility

1. Introduction

Al matrix composites (AMCs) reinforced with particles attract much attention in aerospace and automotive applications, because of their good combination of low density and superior mechanical properties [1]. Compared with micron-sized particles, nanoparticles induce lower stress concentration and avoid strain localization, showing a significant effect on improving the mechanical properties of Al matrix alloys [2]. AMCs reinforced with nanoparticles can be fabricated by stir casting and high energy ball milling [3,4]. Thus, many researchers focus on the effects of nanoparticles on the structure evolution in matrix Al alloys. The plastic deformation is adopted to investigate the structure evolution in AMCs reinforced with nanoparticles, such as hot extrusion and rolling processes [5,6]. The severe plastic deformation techniques are also adopted, including equal channel angular pressing and high-pressure torsion [7,8]. These technologies successfully fabricated AMCs with heterogeneous structures through the addition of nanoparticles, for example, the layered structure and gradient structure, and the increasing strength and ductility were found [9,10]. Among severe plastic deformation techniques, the accumulative roll bonding (ARB) process is more suitable for the production of metallic multi-layer composites in terms of its commercial prospect in industrial fields,

CONTACT Qinglong Zhao zhaoqinglong@jlu.edu.cn; Qichuan Jiang jqc@jlu.edu.cn State Key Laboratory of Automotive Simulation and Control, Jilin University, Changchun, PR People's Republic of China; Key Laboratory of Automobile Materials, Ministry of Education and School of Materials Science and Engineering, Jilin University, No. 5988 Renmin Street, Changchun 130025, PR People's Republic of China

Supplemental data for this article can be accessed here. https://doi.org/10.1080/21663831.2020.1744759

because it can be easily implemented to standard rolling mills. [11–13].

The repetitive rolling cycle of ARB makes it possible to obtain the samples with tailored properties depending on the sandwich-like structure or reinforcements (fibers, foils or particles) [14–16]. In the lamella structure, the soft layer could possess similar strength with the hard layer due to the accumulation of geometrically necessary dislocations in the soft layer during deformation [17,18]. The combination of soft and hard layers is expected to provide an efficient improvement on strength with less reduction of ductility [19]. For AMCs, many works have been carried out to fabricate this kind of ARB composites by adding the particles between the bonding surfaces [20]. However, the matrix alloy and reinforcement particles are hard to get a good bond because of the existence of oxidation film, leading to a decrease in the strengthening effect. On another hand, the lamella structure is difficult to obtain in Al alloys because of the lack of twinning or phase transformation in α-Al. The tensile properties of AMCs reinforced with ceramic particles after ARB are also investigated, and a significant improvement in tensile strength is found [15]. Moreover, nanoparticles have significant impacts on dislocations, leading to different deformation behaviors of AMCs from Al alloys. Considering the nanoparticles can refine the grain structure and impede the grain growth during the recrystallization, it is possible to fabricate the heterogeneous structure by controlling the distribution of nanoparticles [21,22]. Also, it seems to improve the mechanical performance of the matrix Al alloy by utilizing the ARB process with the help of nanoparticles. Thus, it is interesting to design the heterogeneous hierarchical structures in AMCs reinforced with nanoparticles by ARB and to explore the balance between strength and ductility.

In our previous work, 1.0 wt% TiC_p was introduced into the Al-Mg-Si sheet through the master alloy-casting process, and an obvious improvement in tensile performance was obtained [6]. AMCs with a high volume of nanoparticles are hard to get a considerable reinforcing effect of nanoparticles using the traditional fabrication methods due to the cluster of nanoparticles. However, the distribution of nanoparticles is improved to enhance the tensile properties of the matrix Al-Mg-Si alloy in this work. A hierarchical structure is obtained in terms of the grain structure, the distribution of TiC_p and the average size of precipitates. This work proposes a new strategy to fabricate the hierarchically heterogeneous structure to enhance the properties of Al sheets. Also, the processes in this work are suitable for applications in industrial production.

2. Material and methods

2.1. Accumulative roll bonding

The detail fabrication process of the primary materials is provided in the Supplement. ARB process of multi-layered Al-Mg-Si matrix composite reinforced with TiC_p is shown in Figure 1 of the Supplement, which involves three main steps: I. the surface treatment of the matrix layer and the 3.0-TiC_p composite layer which includes degreasing of bonding surfaces by methanol and then brushing the degreased surfaces using a steel brush. II. The two degreased samples (the primary matrix alloy and 3.0-TiC_p composite) were wrapped together with aluminum foil and heat-treated at 550°C for 5 min. III. The prefab was taken out from the furnace and hot-rolled at 500 ± 5°C from 3.2 mm to 1.6 mm. The number of initial layer stacking for ARB is two. The hard alloy was used as lining plates during the hot-rolling process in order to reduce the heat dissipation [23]. These steps were repeated for 5 times, and the detailed description of materials were provided in table 1 of the Supplement. At last, the samples after ARB were aged at 180°C for 5 h.

2.2. Investigation of microstructure and tensile properties

The microstructures were observed through a scanning electron microscope (SEM, Tescan vega3 XM) equipped with electron backscatter diffraction (EBSD, Oxford). EBSD data were processed by using the HKL Channel 5 software, and the critical angles of 2° and 15° were adopted in the boundary detection. The precipitates were observed by transmission electron microscopy (TEM, JEM-2100F). TEM thin foils were prepared at −20°C using twin-jet electropolishing with a solution of 90 vol.% methanol and 10 vol.% perchloric acid at 20 V. The bone-shaped tensile specimens were prepared with a gauge cross-section of $4.0 \times 1.4\ mm^2$ and a gauge length of 10 mm. Tensile tests were performed by a servo-hydraulic material testing system (MTS, MTS810) at room temperature using a constant crosshead speed of 0.18 mm/min (initial strain rate of $3.0 \times 10^{-4}\ s^{-1}$), and at least three samples were tested for each state.

3. Results

3.1. Microstructures

Figure 1(a) indicates that the nanosized TiC_p possess a layered distribution along the rolling direction (RD) in the 32-layer 3.0-TiC_p/M composite. Figure 1(b) indicates that the unindexed regions in Figure 1(c) are

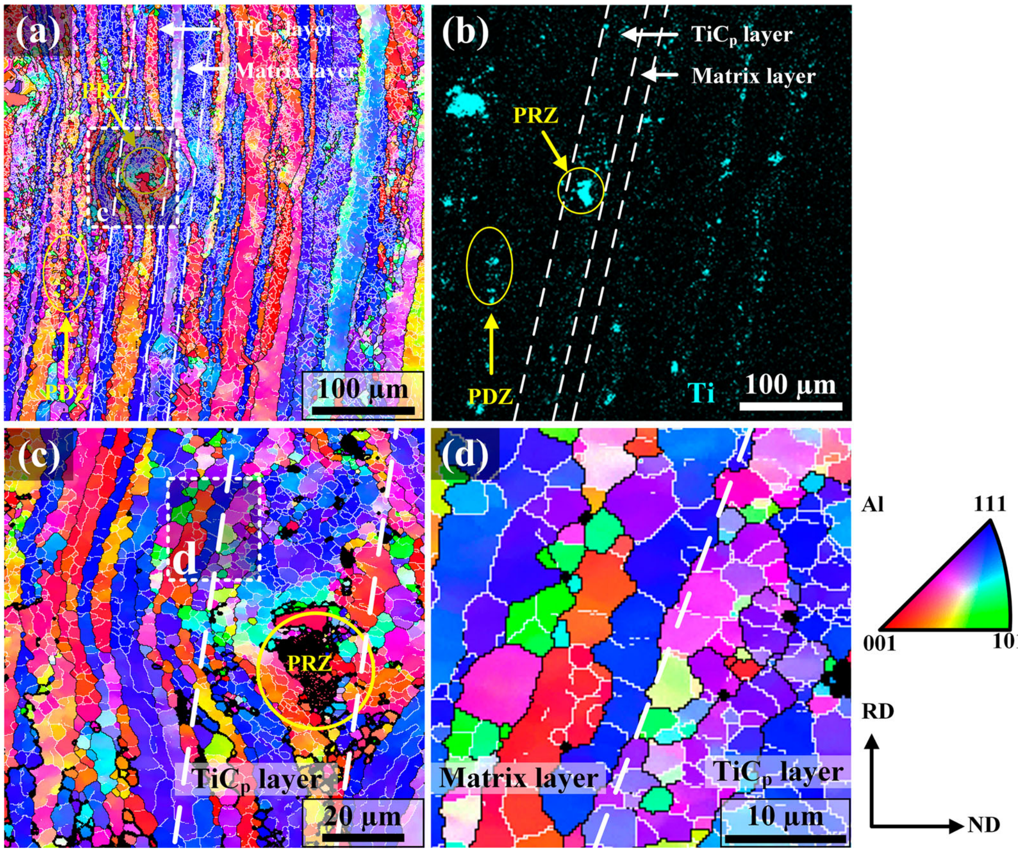

Figure 1. (a) and (b) are the EBSD image and the corresponding EDS results of the same area in the 32-layer 3.0-TiC_p/M composite; (c) the EBSD image of the PRZ and (d) the EBSD image of matrix layer next to the PRZ. The white line represents the sub-grain boundaries.

the agglomeration of TiC_p. These regions are defined as nanoparticles rich zones (PRZ). The regions with relatively dispersed TiC_p are defined as nanoparticle dispersed zones (PDZ) in this paper. In the TiC_p layer, PDZ and PRZ both existed. Distorted deformation zones formed around the PRZ after the ARB process and the grain size in this region was the smallest (Figure 1(c)). It implies that the clusters of TiC_p affected the plastic deformation similarly to microparticles. Figure 1(d) shows the microstructure of the interface between the matrix layer and the TiC_p layer based on the EDS result (Figure 1(b)). The grain size gradually increased from the TiC_p layer to the matrix layer, forming a bimodal-sized grain structure.

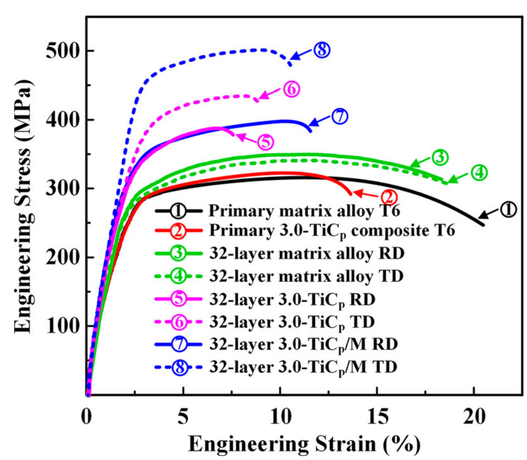

Figure 2. Typical engineering stress-strain curves of the primary Al-Mg-Si matrix alloy, the primary 3.0-TiC_p composite, and the ARB samples.

3.2. Tensile properties

Figure 2 shows the engineering stress–strain curves at room temperature, and the uniform elongation is adopted to compare the material failure in Table 1. Ultimate tensile strength (UTS) and yield strength (YS) increased obviously after the ARB process. The UTS and YS were 501 ± 3 MPa and 443 ± 5 MPa along the TD in 32-layer 3.0-TiC_p/M composite, respectively. They were ∼ 59% and 62% higher than those of the primary matrix alloy T6 (Table 1). The 32-layer 3.0-TiC_p/M composite also showed an outstanding improvement on UTS and YS along the RD (398 ± 5 MPa and 321 ± 3 MPa, respectively). The UTS and YS of 32-layer 3.0-TiC_p composite were 385 and 324 MPa along the RD, and 431 and 380 MPa along the TD. Among the tested samples, the

Table 1. The ultimate tensile strength, yield strength and uniform elongation of the primary Al-Mg-Si matrix alloy, 3.0-TiC_p composite, and ARB samples.

Samples	YS (MPa)	UTS (MPa)	ε_u (%)
Primary matrix alloy	273 ± 4	315 ± 4	10.0 ± 0.5
Primary 3.0-TiC_p composite	274 ± 5	322 ± 4	8.1 ± 0.8
32-layer Matrix RD	280 ± 4	347 ± 3	9.4 ± 0.6
32-layer Matrix TD	262 ± 3	337 ± 9	9.3 ± 0.7
32-layer 3.0-TiC_p RD	324 ± 4	385 ± 4	4.2 ± 0.5
32-layer 3.0-TiC_p TD	380 ± 6	431 ± 5	5.0 ± 0.3
32-layer 3.0-TiC_p/M RD	321 ± 3	398 ± 5	7.4 ± 0.1
32-layer 3.0-TiC_p/M TD	443 ± 5	501 ± 3	6.4 ± 0.6

uniform elongation decreased with the increased tensile strength. However, the decreasing trend was not significant, compared to the increasing trend of tensile strength.

3.3. Precipitates

Precipitation hardening in the 6000 series alloy is obvious. The sequence of precipitation is GP zones → needle-like β'' → rod-shaped β' → hexahedron β, and the needle-like β'' precipitate is the most efficient for strengthening these alloys and provides maximum hardness [24]. The grain size of the PDZ in 32-layer 3.0-TiC_p/M composite is ~1 μm (Figure 3(a)). The needle-shaped β'' precipitates with an average size of 35 nm were observed in the PDZ (Figures 3(b) and (e)). Moreover, the TiC_p could promote the dislocation generation during the hot-rolling, and these dislocations could act as the precipitation nucleation sites of the β'' precipitates (Figure 3(c)). As a result, the TiC_p promoted the formation of β'' precipitates during the aging process.

The length of β'' precipitates was measured to make a better comparison of precipitate sizes. The average lengths of β'' precipitates were 14 and 19 nm near and away from the TiC_p in the PRZ of 32-layer 3.0-TiC_p/M composite, respectively (Figure 4). Due to the interaction between the nanoparticles, the dislocation density was high near TiC_p. These dislocations can promote the precipitation of β'' precipitates as mentioned above, thus leading to the finer β'' precipitates. Due to the small amount of TiC_p in the PDZ and other regions, dislocations generated during the hot rolling were less than those in the PRZ, providing less precipitation sites as compared to the PRZ. Therefore, the average length of β'' precipitates was bigger in the PDZ than that in the PRZ.

4. Discussion

The main reason for the improvement in the tensile strength of the 32-layer TiC_p/M composite is the layered distribution of TiC_p. The extra dislocations and bimodal-sized grain structure caused by TiC_p further lead to bimodal-sized β'' precipitates in the matrix layer and TiC_p layer. Based on the observations in this paper, here a model is proposed to describe the present case of a hierarchically heterogeneous structure in the 32-layer 3.0-TiC_p/M composite (Figure 5). The β'' precipitates

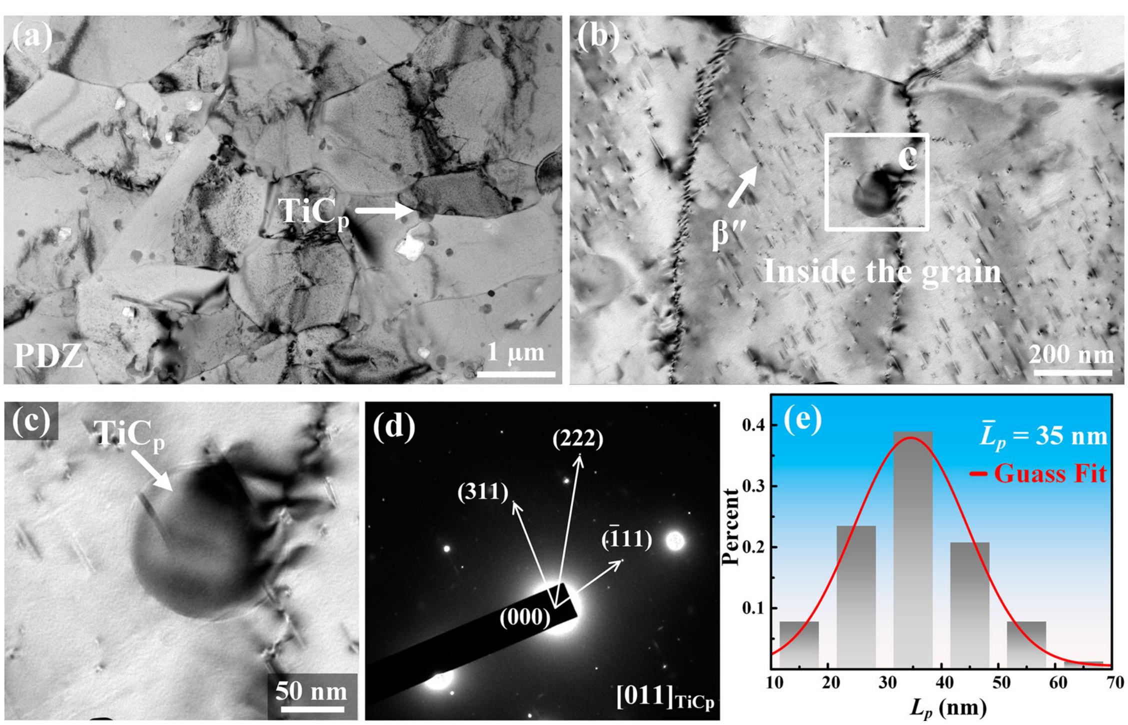

Figure 3. TEM micrographs of the (a) PDZ, (b) the β'' precipitates and (c) the nanosized TiC_p inside the PDZ; (d) the corresponding selected-area diffraction pattern; (e) the distribution of the length of β'' precipitates.

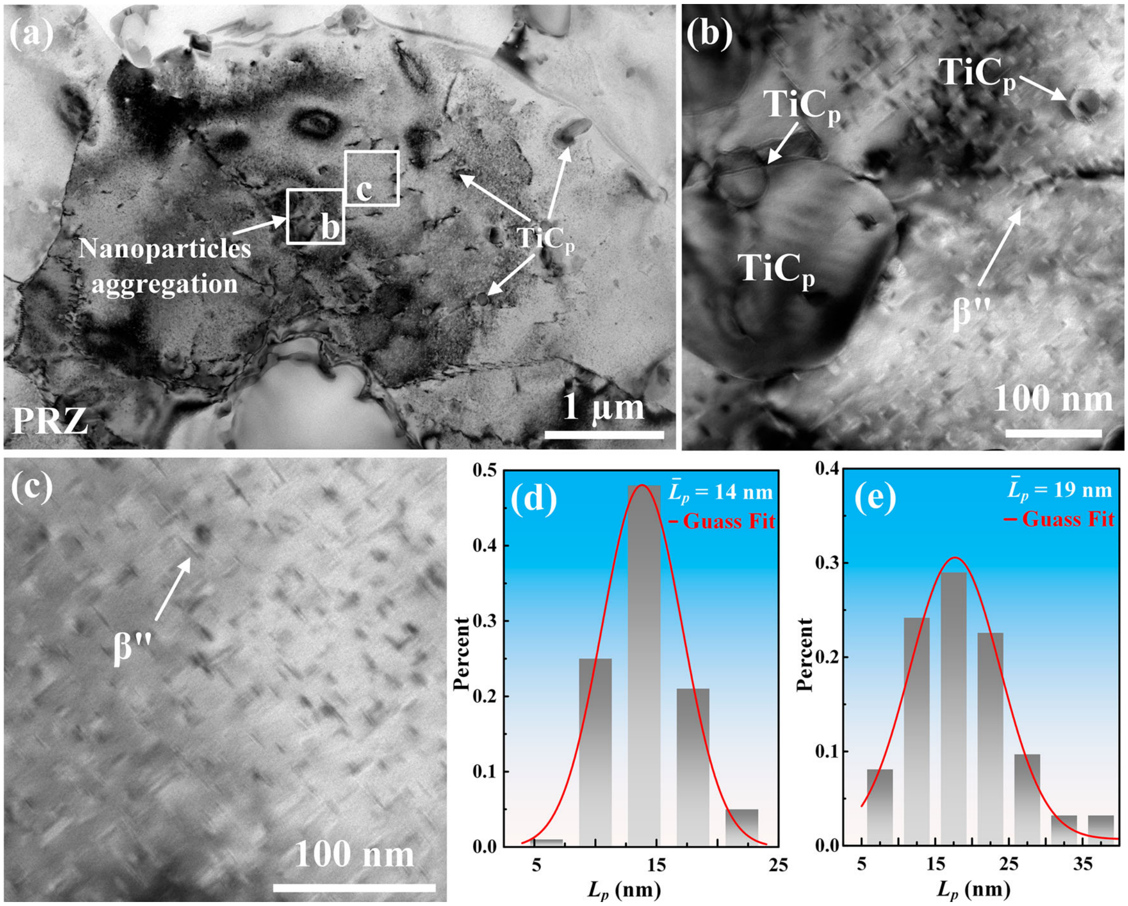

Figure 4. TEM micrographs of (a) the PRZ, (b) the aggregation of the nanoparticles region and (c) the region next to nanoparticles aggregation region in the PRZ; (d) and (e) are the distributions of the lengths of β'' precipitates in these two regions, respectively.

show finer sizes in the TiC_p layer, compared to the matrix layer (Figure 5). The average length of β'' precipitates reduced as the number per unit volume increases, because of the constant solute content. During the aging process, the extra dislocations caused by the nanosized TiC_p act as the heterogeneous precipitation nucleation sites of the β'' precipitates, leading to a larger amount of fine β'' precipitates in the TiC_p layer. Hence, the nanosized TiC_p promote the formation and reduce the average length of β'' precipitates. The finer β'' precipitates impede the movement of dislocations and lead to a larger value of the Orowan stress. Besides, the fine grain size can also contribute to the yield strength according to the Hall-Petch equation: $\bar{\sigma}_{HP} = k/\sqrt{d}$ [25].

The difference in grain sizes and β'' precipitate lengths further causes the different strengths between the TiC_p layer and the matrix layer. The matrix layer and TiC_p layer together form a layered structure with discrepant strengths. During tension, the TiC_p layer with finer grains and precipitates is capable of providing high strength. Meanwhile, the matrix layer with coarser grains and precipitates is easier to deform due to lower yield strength and possesses relatively higher strain hardening

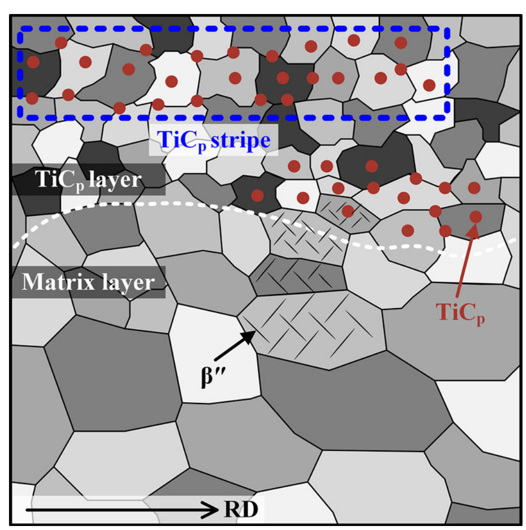

Figure 5. Schematic illustration of the hierarchical structure in the 32-layered 3.0-TiC_p/M composite.

capability. It was also reported that more energy would be dissipated during the crack propagation when lamellar ductile domains were used. Stronger back-stress work hardening and more energy dissipation during tensile tests were conducive to higher strength and ductility [17]. For heterogeneous lamella structures consisting of domains with different strengths, the soft layers (matrix layers) can possess similar strength with the hard layers (TiC_p layers) due to the accumulation of geometrically necessary dislocations (GNDs) in the soft layers during deformation, and the global yield strength can be even higher than that obtained in the uniform grain structure [17,18]. The heterogeneous structure is observed to produce an intrinsic synergetic strengthening, with its tensile strength much higher than that calculated by the rule of the mixture from separate layers, which is attributed to the macroscopic stress gradient and plastic incompatibility between layers [26,27]. For hierarchically structured metals with stable heterogeneous structures, their high ductility is attributed to extra strain hardening due to the presence of strain difference and the change of stress states, which generates GNDs and promotes the generation and interaction of dislocations [28]. As a result, the TiC_p layer with a heterogeneous structure (PDZ and PRZ) provides extra strengthening effects.

5. Conclusions

In this paper, a laminated composite composed of Al-Mg-Si matrix alloy and nanosized TiC_p/Al-Mg-Si composite was fabricated by the accumulative roll bonding process.

The hierarchical heterogeneous structure showed a more significant strengthening effect and better strength-ductility balance than the conventional laminated structure. The combination of the TiC_p layer and the matrix layer provided an extra shear force to disperse the nanoparticles, leading to the enhancement of strength. The hierarchical structure in 3.0-TiC_p/M composite increased the yield strength (from 380 MPa to 443 MPa) with no loss in uniform elongation (from 5.0% to 6.4%), compared to the 32-layered 3.0-TiC_p composite. The strength anisotropy in composites was resulted by the distribution of TiC_p stripe in the TiC_p layer. Moreover, this work provides a new strategy for hierarchical microstructural design to achieve high strength of laminated nanocomposites, which is a promising method for industrial production.

Disclosure statement

No potential conflict of interest was reported by the author(s).

Funding

This work was funded by the National Natural Science Foundation of China [grant number 51790483] and the ‘thirteenth five-year plan’ Science & Technology Research Foundation of Education Bureau of Jilin Province, China [grant number JJKH20190133KJ].

ORCID

Qinglong Zhao http://orcid.org/0000-0002-7124-4032

References

[1] Jo MC, Choi JH, Yoo J, et al. Novel dynamic compressive and ballistic properties in 7075-T6 Al-matrix hybrid composite reinforced with SiC and B4C particulates. Compos Part B Eng. 2019;174:107041.
[2] Tian WS, Zhou DS, Qiu F, et al. Superior tensile properties of in situ nano-sized TiCp/Al-Cu composites fabricated by reaction in melt method. Mater Sci Eng A. 2016;658:409–414.
[3] Geng R, Qiu F, Jiang QC. Reinforcement in Al matrix composites: a review of strengthening behavior of nano-sized particles. Adv Eng Mater. 2018;20:1701089.
[4] Geng R, Tian WS, Zhao QL, et al. Superior cryogenic tensile strength and ductility of in situ Al-Cu matrix composite reinforced with 0.3 wt% nano-sized TiCp. Adv Eng Mater. 2018;20:1701137.
[5] Wang L, Qiu F, Zhao Q, et al. Superior high creep resistance of in situ nano-sized TiCx/Al-Cu-Mg composite. Sci Rep. 2017;7:1–10.
[6] Geng R, Qiu F, Zhao QL, et al. Effects of nanosized TiCp on the microstructure evolution and tensile properties of an Al-Mg-Si alloy during cold rolling. Mater Sci Eng A. 2019;743:98–105.
[7] Sabirov I, Kolednik O, Valiev RZ, et al. Equal channel angular pressing of metal matrix composites: effect on particle distribution and fracture toughness. Acta Mater. 2005;53:4919–4930.
[8] Housaer F, Beclin F, Touzin M, et al. Interfacial characterization in carbon nanotube reinforced aluminum matrix composites. Mater Charact. 2015;110:94–101.
[9] Huang LJ, Geng L, Peng HX. Microstructurally inhomogeneous composites: is a homogeneous reinforcement distribution optimal? Prog Mater Sci. 2015;71:93–168.
[10] Zhao Y, Massion R, Grosdidier T, et al. Gradient structure in high pressure torsion compacted iron powder. Adv Eng Mater. 2015;17:1748–1753.
[11] Chaudhari GP, Acoff V. Cold roll bonding of multi-layered bi-metal laminate composites. Compos Sci Technol. 2009;69:1667–1675.
[12] Ivanov K V, Fortuna S V, Kalashnikova TA, et al. Effect of alumina nanoparticles on the microstructure, texture, and mechanical properties of ultrafine-grained aluminum processed by accumulative roll bonding. Adv Eng Mater. 2019;21:1701135.
[13] Bagherpour E, Reihanian M, Miyamoto H. Tailoring particle distribution non-uniformity and grain refinement in nanostructured metal matrix composites fabricated by severe plastic deformation (SPD): a correlation with flow stress. J Mater Sci. 2017;52:3436–3446.
[14] Alizadeh M, Dashtestaninejad MK. Development of Cu-matrix, Al/Mn-reinforced, multilayered composites by accumulative roll bonding (ARB). J Alloys Compd. 2018;732:674–682.
[15] Alizadeh M, Paydar MH, Sharifian Jazi F. Structural evaluation and mechanical properties of nanostructured

Al/B4C composite fabricated by ARB process. Compos Part B Eng. 2013;44:339–343.
[16] Alizadeh M, Paydar MH. Fabrication of nanostructure Al/SiCP composite by accumulative roll-bonding (ARB) process. J Alloys Compd. 2010;492:231–235.
[17] Zan YN, Zhou YT, Liu ZY, et al. Enhancing strength and ductility synergy through heterogeneous structure design in nanoscale Al2O3 particulate reinforced Al composites. Mater Des. 2019;166:107629.
[18] Wu X, Yang M, Yuan F, et al. Heterogeneous lamella structure unites ultrafine-grain strength with coarse-grain ductility. Proc Natl Acad Sci. 2015;112:14501–14505.
[19] Wu X, Zhu Y. Heterogeneous materials: a new class of materials with unprecedented mechanical properties. Mater. Res Lett. 2017;5:527–532.
[20] Jafarian H, Habibi-Livar J, Razavi SH. Microstructure evolution and mechanical properties in ultrafine grained Al/TiC composite fabricated by accumulative roll bonding. Compos Part B Eng. 2015;77:84–92.
[21] Li Q, Qiu F, Dong B, et al. Fabrication, microstructure refinement and strengthening mechanisms of nanosized SiCp/Al composites assisted ultrasonic vibration. Mater Sci Eng A. 2018;735:310–317.
[22] Wang L, Qiu F, Zhao QL, et al. Simultaneously increasing the elevated-temperature tensile strength and plasticity of in situ nano-sized TiCx/Al-Cu-Mg composites. Mater Charact. 2017;125:7–12.
[23] Zha M, Meng X-T, Zhang H-M, et al. High strength and ductile high solid solution Al-Mg alloy processed by a novel hard-plate rolling route. J Alloys Compd. 2017;728:872–877.
[24] Ding L, Jia Z, Nie J-F, et al. The structural and compositional evolution of precipitates in Al-Mg-Si-Cu alloy. Acta Mater. 2018;145:437–450.
[25] Aversa A, Marchese G, Lorusso M, et al. Microstructural and mechanical characterization of aluminum matrix composites produced by laser powder bed fusion. Adv Eng Mater. 2017;19:1700180.
[26] Wu XL, Jiang P, Chen L, et al. Synergetic strengthening by gradient structure. Mater Res Lett. 2014;2:185–191.
[27] Wu X, Jiang P, Chen L, et al. Extraordinary strain hardening by gradient structure. Proc Natl Acad Sci. 2014;111:7197–7201.
[28] Xu R, Fan G, Tan Z, et al. Back stress in strain hardening of carbon nanotube/aluminum composites. Mater Res Lett. 2018;6:113–120.